Adding Mean Sea Surface (MSS) as an Altimetry Product

David T. Sandwell, August 1, 2022, (mss_sio_32.1.nc)

Introduction

Our standard SIO altimetry processing products include; east and north deflections of the vertical, free-air anomaly, and vertical gravity gradient. The approach uses the EGM2008 global geopotential model [*Pavlis et al.,* 2012] as a reference in a classic remove/restore processing chain. Here we add the mean sea surface height as an additional product. To begin we need to update the global dynamic ocean topography (DOT) by taking the difference between MSS_CLS22 [*Schaeffer et al.,* 2022] and the EGM_mean_tide geoid. This new DOT with respect to EGM2008 was low-pass filtered at 120 km wavelength (Figure 1). We add this to the EGM2008 geoid to update the geopotential model.

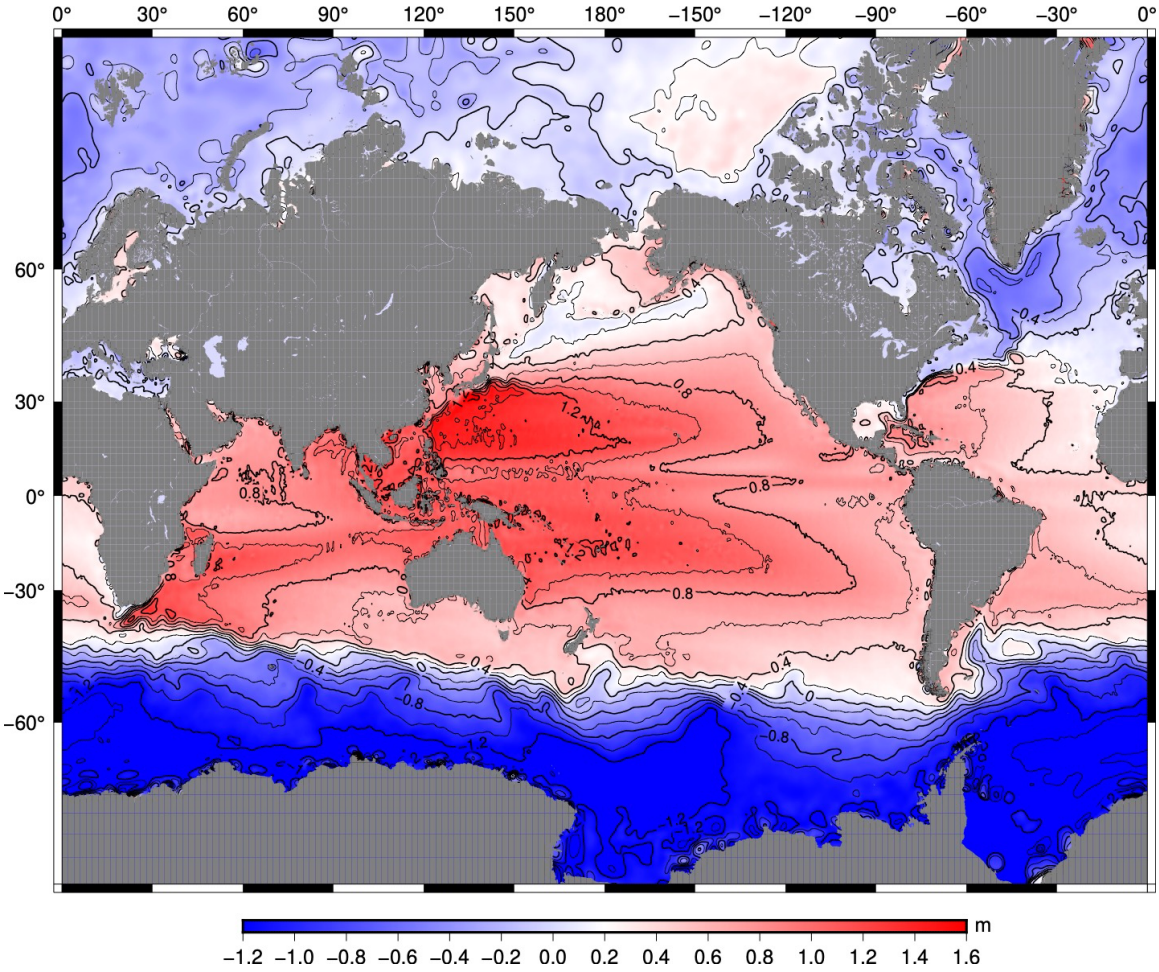

Figure 1. The MSS_CLS21 model minus the GEOID_EGM model. The difference (i.e., dynamic ocean topography DOT) was low-pass filtered at 117 km. The median difference is 0.381 m and the median absolute deviation is 0.565 m. Note these statistics included the DOT data extended onto land.

As usual, we remove the MSS_EGM_CLS22, updated with CLS22, estimates from the MSS_CLS22 to form residual heights. Only heights with acceptable uncertainties < 8 cm are used. We combine these height data and uncertainties with dense slope data from all the SIO retracked products to form the usual residual east and north slope grids with respect to MSS_EGM_CLS22 to form new residual height grid. We add the MSS_EGM_CLS22 grid to the residual height grid to form a new, higher resolution, MSS_CLS22_updated grid. This document provides a detailed analysis of the development of the new MSS_CLS22_updated grid.

Difference between CLS and EGM products

To understand the issues related to this analysis we first construct maps of the difference between the MSS from the CLS22 and EGM_ products. The starting grids are:

MSS_CLS22_1s60_Etp.xyz - The 2022 MSS from CLS.

ErMSS_CLS21_1s60_Etp.xyz - The 2021 ERR grid from CLS

geoid.egm2008_MeanTide.grd – The EGM2008 geoid computed with a mean tide.

dot.cls22.grd – Mean dynamic topography associated with this model (described below).

ssh.egm2008.cls22.grd = geoid.egm2008_MeanTide.grd + dot.cls22.grd

As a first sanity check we evaluate the difference mss.cls22.grd - ssh.egm2008.cls22.grd . This is shown in Figure 2. The differences are very small and reflect the low-pass filtering of the dot.cls22.grd.

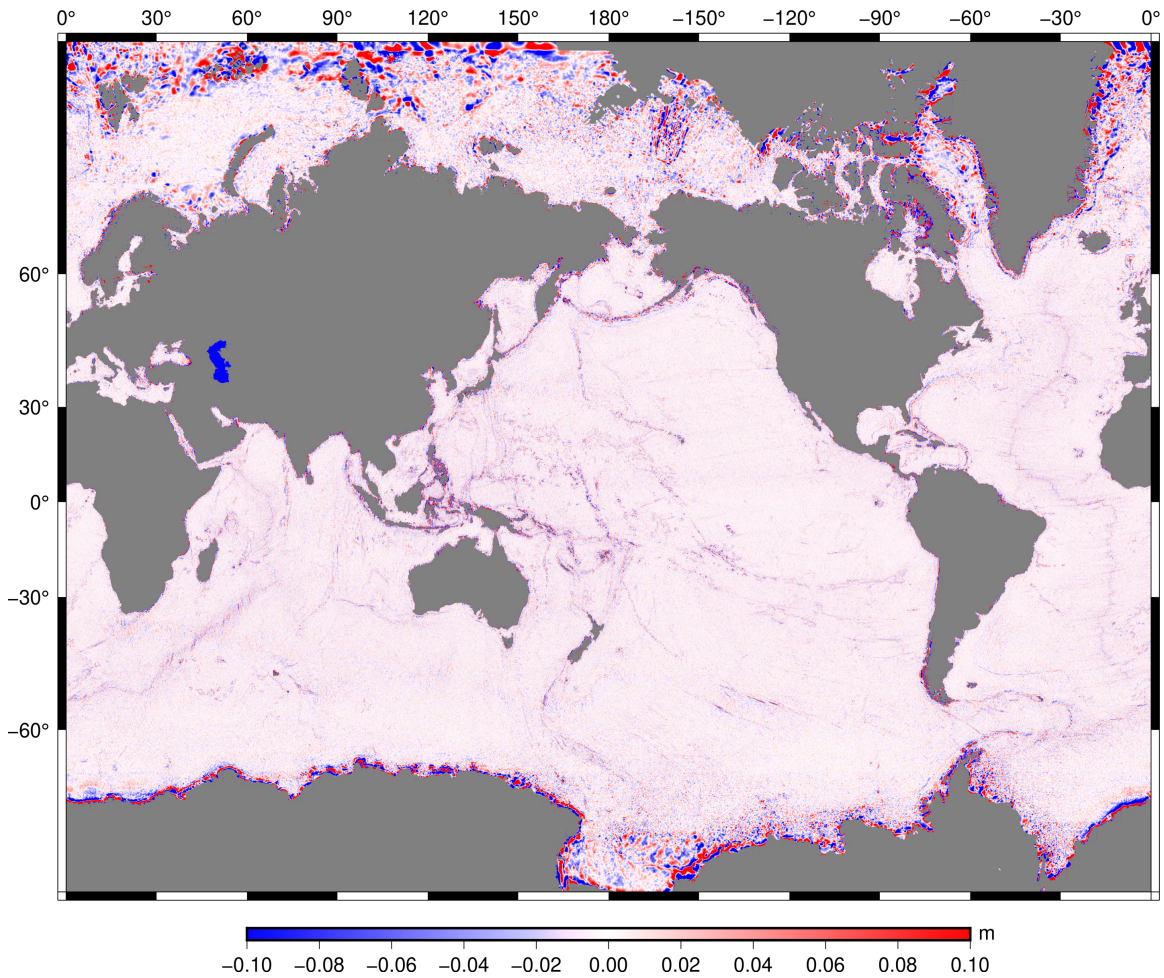

Figure 2. Difference between the MSS_CLS22 grid and the MSS_EGM_CLS22 updated grid. The median difference is -0.0003 m and the median absolute deviation is 0.012 m. The differences are all due to low-pass filtering the DOT that went into the MSS_EGM_CLS21.

Remove/Restore Gridding Method

The method tested for constructing a higher resolution MSS grid has the following algorithm. Extract height and uncertainties (ERR) data from the MSS_CLS22 – MSS_EGM_CLS22 grid shown in Figures 2. These form the residual height data and uncertainties. Next assemble all the along-track slope data in the SIO data base. These are processed as described in *Sandwell et al.,* [2021]. Note that a slope correction [*Sandwell and Smith,* 2014] has been applied to the CLS22 height data as well as the all the along-track slope data. Also, the along-track slope data have the MSS_EGM_CLS22 slopes removed. These height/standard deviations and slope data are combined in the *img_interp_ht* program using biharmonic splines in tension [*Wessel and Bercovici*, 1998].

We first do this using the actual uncertainties given in the ERR_CLS22 grid. A threshold of 8 cm ERR is used to eliminate less certain data. We found that when gridding the heights and slopes together that they are somewhat inconsistent. The height data are smoother than the slope data so using the CLS height constraint lowers the amplitude of the output vertical deflection grids with respect to gridding done when there are no height constraints. Table 1 shows some amplitudes of the east component of vertical deflection in microradian at selected points. This evaluation illustrates the trade-off between fitting the original slope data and fitting the new height data. When the height data are used with their original 1-sigma uncertainty, the gridded slopes are significantly smaller than the slopes when no height data are used. When the height data are used with the 2Xsigma uncertainties then the slopes have a better match to the unconstrained slopes. When the height data are used with the 100Xsigma uncertainties then the slopes match the original slope grids exactly.

Table 1. East component of deflection of the vertical in microradian at selected points for various multiples of uncertainty for the CLS15 height data.

x	y	slope data only	1σ heights	2σ heights	100σ*
54	362	15.78	15.78	15.78	15.78
77	1106	14.53	5.78	8.91	14.53
309	2426	12.03	6.40	7.65	12.03
537	4281	15.78	12.65	13.90	15.78
193	5465	14.53	12.65	13.90	14.53

* Note that 100 σ provides a very blocky and poor fit to the height data while there is a perfect fit to the slope data.

The height differences between the new MSS_CLS22_updated and the original MSS_CLS22 are shown in Figure 3 for the 2X height uncertainties. As expected, the differences are small except in areas of very small-scale geoid anomalies at seamounts and ridges.

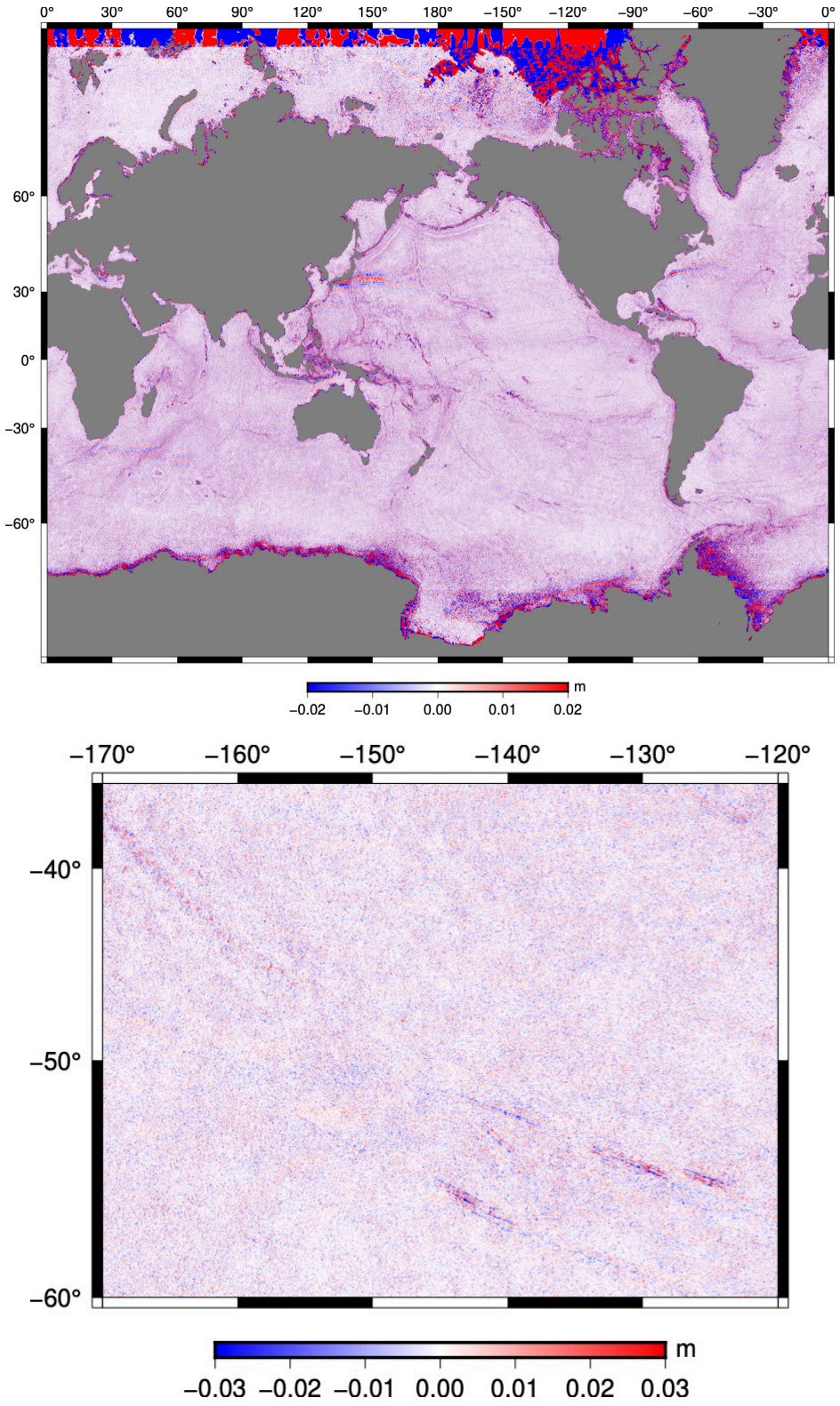

Figure 3. (top)The difference between the new MSS_CLS22_updated grid and the original MSS_CLS22 grid. The box is the area where misfit were evaluated. (bottom) difference between updated and original CLS grid in the South Pacific.

We computed the mean standard deviation for the difference between the new MSS_CLS21_updated and the MSS_CLS21 grid for a large area of the South Pacific (-

R190/240/-60/-35, box in Figure 3) for a number of cases (Table 2). We decomposed the difference into a high-pass filtered grid and a low pass filtered grid using a Gaussian filter with a 0.5 gain at 60 km. As expected most of the mean difference goes into the low pass and most of the standard deviation is in the high-pass.

Table 2 Statistics on the difference between the updated MSS and the CLS MSS for South Pacific area (-R190/240/-60/-35)

description	mean (mm)	std (mm)
2X sigma on height data	-0.04	5.4
2X sigma, high-pass (60 km)	.00004	5.1
2X sigma, low-pass (60 km)	-0.5	1.0

Comparison of MSS_CLS22_updated with MSS_CLS15_updated.

Here we compare the MSS_CLS22_updated with the older MSS_CLS_15_updated to see the possible improvements. Note that the CLS22 model uses more data than the CLS15 model. Much of this is non-repeat altimeter data from CryoSAT-2 and Sentinel-3A/B. Moreover, the CLS22 grid height data were corrected for the geoid slope effect. In addition, the CLS15 grid was updated several years ago when there was less SIO slope data from several altimeters. Thus, we expect that the accuracy and precision of the new model will be superior. A global comparison of the two models is shown in Figure 4. The mean and rms differences for the Pacific area (-R190/240/-60/-35) are -.4 mm and 4.9 mm respectively. A zoom of the Aleutian region reveals some of the details of the differences (Figure 5). Now the low-pass filtered differences (Figure 5b) roughly match the slope correction (Figure 5c). This is expected since both the CLS22 height data and the and the SIO slope data have been corrected for the slope effect which is always positive and the CLS15 modes was not corrected for the slope effect.

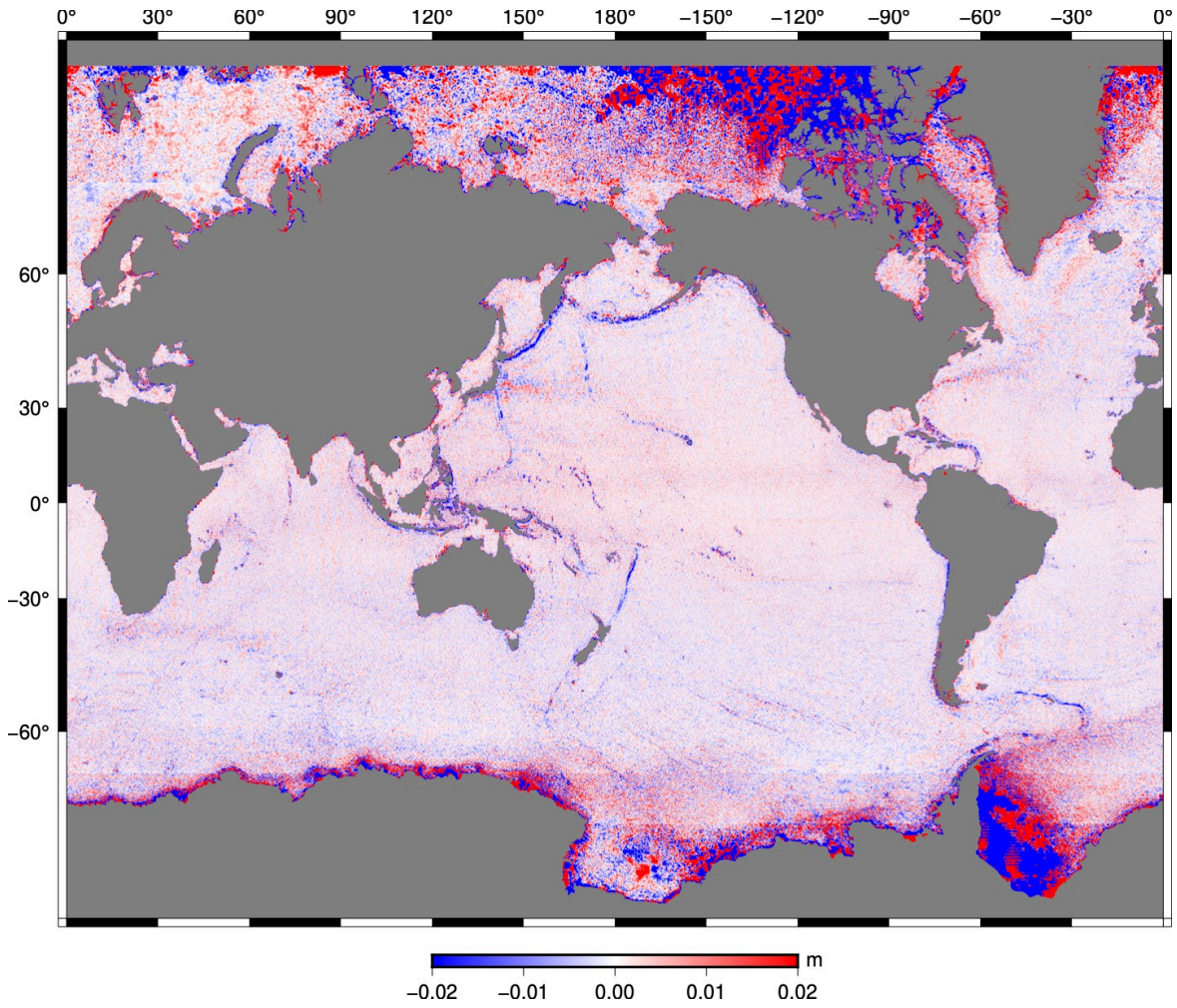

Figure 4. Difference between the 2022 and 2015 CLS models that were both updated with slope data from SIO.

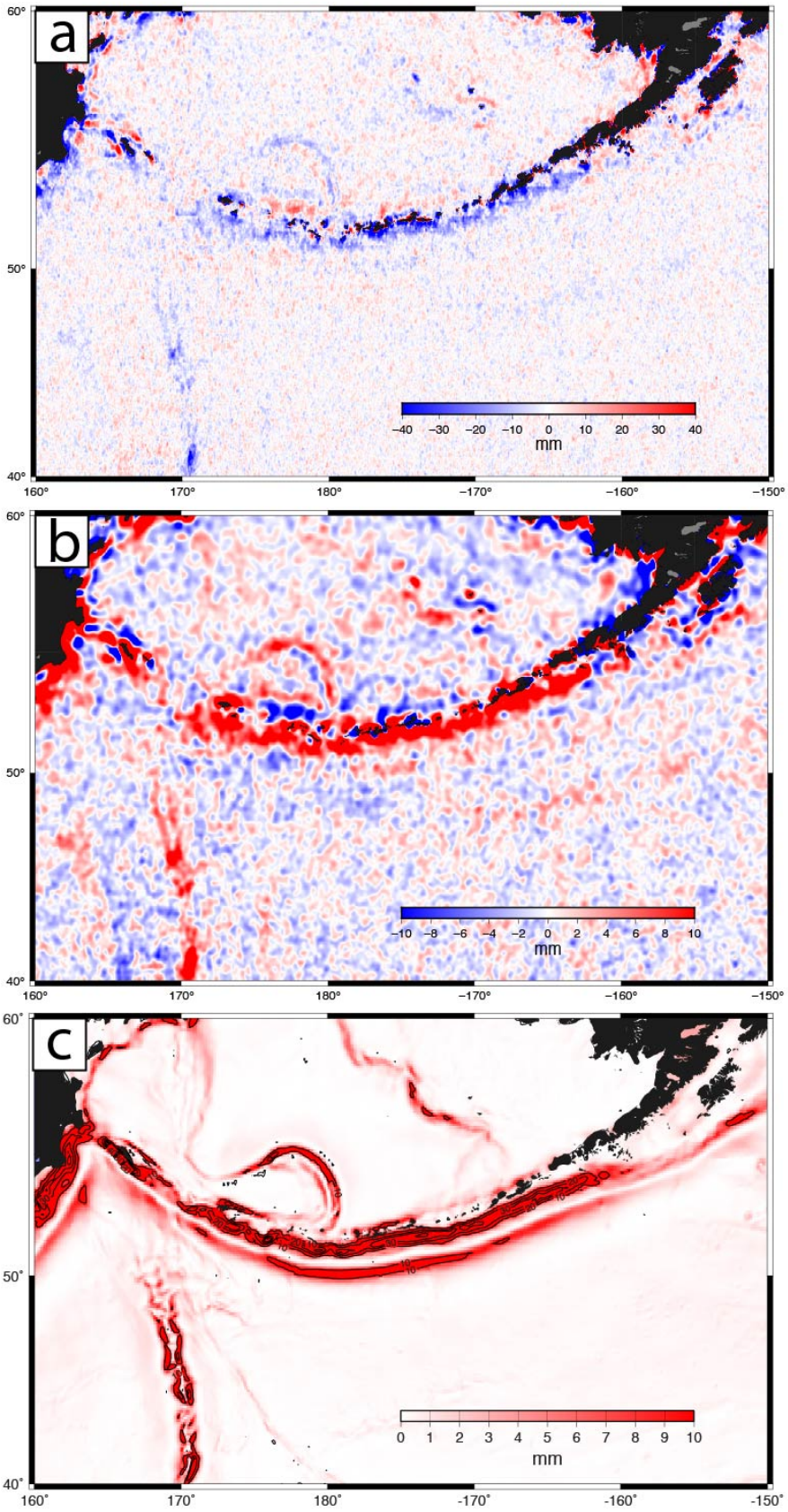

Figure 5. Height difference between new MSS_CLS22_updated and old MSS_CLS15_updated for the Aleutian trench area where map (a) is full difference and (b) is low-pass filtered and sign reversed.

(c) Height correction needed to be applied to radar altimetry data (1000 km altitude) caused by the off-nadir reflection point in areas of large geoid slope.

Conclusions

We have used the along-track slope data from multiple satellites to tune the CLS22 MSS model. The approach uses a biharmonic spline in tension [*Wessel and Bercovici*, 1998] to combine the S&S slope data with the height data. The updated grid has small differences from the original grid with a mean difference of -0.1 mm and standard deviation of 5.4 mm. We deliver this new MSS grid back to CLS for testing and evaluation in the original CLS format.

References

Pavlis, Nikolaos K., Simon A. Holmes, Steve C. Kenyon, and John K. Factor. "The development and evaluation of the Earth Gravitational Model 2008 (EGM2008)." *Journal of Geophysical Research: Solid Earth 117*, no. B4 (2012).

Sandwell, D. T., Harper, H., Tozer, B., & Smith, W. H. (2021). Gravity field recovery from geodetic altimeter missions. Advances in Space Research, 68(2), 1059-1072.

Sandwell, David T., R. Dietmar Müller, Walter HF Smith, Emmanuel Garcia, and Richard Francis. "New global marine gravity model from CryoSat-2 and Jason-1 reveals buried tectonic structure." *Science 346*, no. 6205 (2014): 65-67.

Sandwell, David T., and Walter HF Smith. "Slope correction for ocean radar altimetry." *Journal of Geodesy 88*, no. 8 (2014): 765-771.

Schaeffer, P.; Pujol, M.-I.; Veillard, P.; Faugere, Y.; Dagneaux, Q.; Dibarboure, G.; Picot, N. The CNES CLS 2022 Mean Sea Surface: Short Wavelength Improvements from CryoSat-2 and SARAL/AltiKa High-Sampled Altimeter Data. Remote Sens. 2023, 15, 2910. https://doi.org/10.3390/rs15112910

Wessel, Paul, and David Bercovici. "Interpolation with splines in tension: a Green's function approach." *Mathematical Geology 30*, no. 1 (1998): 77-93.